Biophysical Chemistry 185 (2014) 1–7

Contents lists available at ScienceDirect

Biophysical Chemistry

journal homepage: http://www.elsevier.com/locate/biophyschem

A thermodynamic study of the third PDZ domain of MAGUK neuronal protein PSD-95 reveals a complex three-state folding behavior

Javier Murciano-Calles [a,*], Jose C. Martinez [a], Marta Marin-Argany [b], Sandra Villegas [b], Eva S. Cobos [a,*]

[a] Departamento de Química Física e Instituto de Biotecnología, Facultad de Ciencias, Universidad de Granada, 18071 Granada, Spain
[b] Departament de Bioquímica I Biología Molecular, Facultat de Biociències, Universitat Autónoma de Barcelona, Bellaterra, Barcelona, Spain

HIGHLIGHTS

- Deletion of C-terminal α3-helix of PSD95-PDZ3 changes domain unfolding at neutral pH.
- Calorimetric analysis shows an intermediate state which self-associates upon heating.
- A stabilization of the intermediate occurs when α3-helix is removed.
- CD, FTIR and DLS data also support calorimetric results.
- Folding process becomes more complex when α3-helix is removed.

GRAPHICAL ABSTRACT

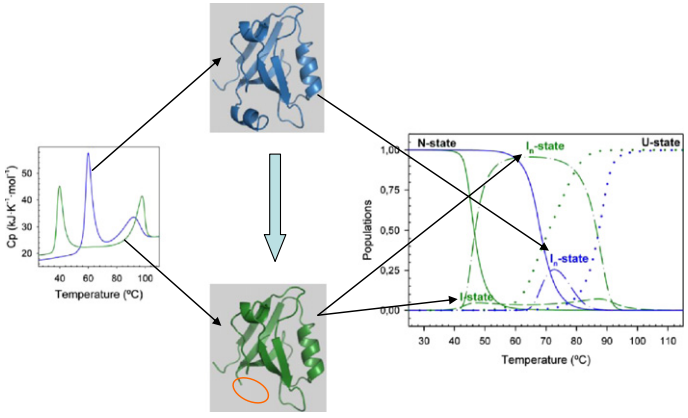

ARTICLE INFO

Article history:
Received 11 September 2013
Received in revised form 17 October 2013
Accepted 21 October 2013
Available online 2 November 2013

Keywords:
PDZ domain
Oligomeric intermediate
Differential scanning calorimetry
Three-state model
Thermodynamics
Protein folding

ABSTRACT

The relevance of the C-terminal α helix of the PDZ3 domain of PSD95 in its unfolding process has been explored by achieving the thermodynamic characterization of a construct where the sequence of the nine residues corresponding to such motif has been deleted. Calorimetric traces at neutral pH require the application of a three-state model displaying three different equilibrium processes in which the intermediate state self-associates upon heating, being stable and populated in a wide temperature range. Temperature scans followed by circular dichroism, Fourier transform infrared spectroscopy and dynamic light scattering support the presence of such oligomeric-partially folded species. This study reveals that the deletion of the α3-helix sequence results in a more complex description of the domain unfolding.

1. Introduction

Important biological processes are based on interaction networks, which contain highly connected nodes, called hub proteins [1]. These hub proteins interact with multiple partners, playing a key role in the network since they allow a fast and efficient way of signaling. The most common modular family present in hub proteins is the PDZ domains. They have a common tri-dimensional organization based on a β barrel integrated by six or seven β strands (β_1, β_2…) surrounded by two α helices [2]. However, there is a significant degree of variability in these domains related to the length and composition of the loops

* Corresponding authors. Tel.: +34 958241000x20284; fax: +34 958272879.
E-mail addresses: jmurciano@ugr.es (J. Murciano-Calles), evasan@ugr.es (E.S. Cobos).

0301-4622/$ – see front matter © 2013 Elsevier B.V. All rights reserved.
http://dx.doi.org/10.1016/j.bpc.2013.10.005

and turns and the N- and C-termini. Another common feature of PDZ domains is their ability to bind a variety of proteins via their C-termini. One prototypic protein family containing PDZ domains is the MAGUK family, which contains three N-terminal PDZ, one SH3 and one GK (guanylate kinase) domains. Among MAGUK proteins, PSD95 (post-synaptic density protein-95) controls the organization and clustering of synaptic signaling complexes, also coordinating the dynamic trafficking that takes place in the synapse [3]. Those polyvalent functions are possible due to its modular distribution, which confers a high degree of conformational plasticity where their domain dynamics is crucial to bind to multiple partners [4]. In particular, the third PDZ domain of PSD95 is followed by an α helix [5] which has been commonly considered as part of such PDZ domain. However, PDZ domains contain only two α-helices, being the third one a linker between the third PDZ and the SH3 domain of PSD95. The role of this helix is crucial, since it mediates interactions between the domains that connect [4]. Thus, its removal means a significant loss of affinity in the binding of the PSD95-PDZ3 domain [6].

Considering the relevance of this α-helix, we have cloned a construct containing residues 302–392 of PSD95 (PSD95-PDZ3$^{302-392}$), where the nine C-terminal residues (EEYSRFEAK) that constitute such helix have been eliminated. We have explored by differential scanning calorimetry (DSC) the effects of its removal in the unfolding process of the domain. Our results, supported by circular dichroism (CD), Fourier transform infrared spectroscopy (FTIR) and dynamic light scattering (DLS) data reveal a complex folding behavior, where a self-associated intermediate state appears. Furthermore, the comparison of this calorimetric analysis with our previous characterization carried out with the domain including the helix (residues 302–402) [7] reveals that the unfolding of the domain becomes a more complex process when the extra C-terminal α3-helix is removed, which opposes the well known correlation between folding complexity and protein size [8].

2. Materials and methods

PSD95-PDZ3$^{302-392}$ domain, including residues 302 to 392 in PSD95 numbering, was sub-cloned into pBAT4 vector (EMBL Core Purification Facility) and expressed in *Escherichia coli BL21/DE3* cells. Protein purification was carried out as previously described [9]. We obtained 8 mg of highly pure protein per liter of LB culture. MALDI-TOF experiments achieved at the Scientific Instrumentation Services (CIC) of the University of Granada confirmed a molecular mass of 9898 Da and ensured purity of the protein. The concentration of protein was measured by spectroscopic measurements, using an extinction coefficient of 1425 $cm^{-1}\cdot M^{-1}$, determined at 278 nm as described [10].

Experimental samples were always prepared by extensive dialysis against 50 mM K-phosphate buffer at pH 7.5 and 4 °C. Differential scanning calorimetry (DSC) experiments were performed in a VP-DSC instrument from Microcal Inc. as described previously [11]. Dynamic light scattering (DLS), Fourier transform infrared spectroscopy (FTIR) and circular dichroism (CD) experiments were conducted as described elsewhere [12–14]. The molecular weight of the different species was calculated from their measured hydrodynamic radii using the DynaPro DYNAMICS 6 software (Wyatt Technology Corporation, USA) considering a globular protein model.

The three-state model including two equilibriums with an oligomeric intermediate ($N \rightleftarrows I_n \rightleftarrows U$), initially used to analyze the calorimetric traces has been described previously [15]. The more complex three-state model displaying three equilibriums comprises three conformational states plus the self-association of one of them. Thus, if we assume that the intermediate state self-associates with a certain n stoichiometry, we obtain the following scheme:

$$\begin{array}{c} N \rightleftarrows I \rightleftarrows U \\ \uparrow\downarrow \\ 1/n\ I_n. \end{array} \tag{1}$$

Thus, there are three equilibrium processes: the first one corresponding to $N \rightleftarrows I$, with a K_{N-I} equilibrium constant; the second one to the complete domain unfolding, $I \rightleftarrows U$, whose equilibrium constant is K_{I-U}, and the third one, to the association equilibrium $I \rightleftarrows (1/n)\ I_n$, whose equilibrium constant is defined by K_{I-In}.

The populations of the native, intermediate, oligomeric intermediate and unfolded states (named as f_N, f_I, f_{In} and f_U respectively), can be calculated as a function of the total protein concentration, P, by means of the following expressions:

$$\begin{aligned} f_N &= \frac{[N]}{P} \rightarrow [N] = f_N \cdot P \\ f_U &= \frac{[U]}{P} \rightarrow U = f_U \cdot P \\ f_I &= \frac{[I]}{P} \rightarrow [I] = f_I \cdot P \\ f_{In} &= \frac{n[I_n]}{P} \rightarrow [I_n] = f_{In} \cdot \frac{P}{n}. \end{aligned} \tag{2}$$

Since the sum of the populations of the conformational states has to be equal to the unit ($f_N + f_I + f_U + f_{In} = 1$), the next equation can be easily deduced:

$$[I_n] = (1 - f_N - f_U - f_I) \cdot \frac{P}{n}. \tag{3}$$

The equilibrium constants can be defined as a function of the populations as follows:

$$K_{N-I} = \frac{[I]}{N} = \frac{f_I}{f_N} K_{I-U} = \frac{[U]}{I} = \frac{f_U}{f_I} K_{I-In} = \frac{[I_n]^{1/n}}{[I]}. \tag{4}$$

By replacing Eq. (3) in the last expression, we obtain:

$$K_{I-In} = \frac{[I_n]^{1/n}}{I} = \frac{\left(\frac{f_{In} \cdot P}{n}\right)^{1/n}}{f_I \cdot P} \rightarrow K_{I-In} = \frac{f_{In}^{1/n} \cdot P^{1/n}}{f_I \cdot n^{1/n} \cdot P}. \tag{5}$$

And, by reorganizing this expression, we will finally get:

$$f_{In}^{1/n} = K_{I-In} \cdot f_I \cdot n^{1/n} \cdot \frac{P}{P^{1/n}} \rightarrow f_{In} = K_{In}^n \cdot f_I^n \cdot n \cdot P^{n-1}. \tag{6}$$

Besides, since $f_{In} = (1 - f_N - f_U - f_I)$ and, taking into account that $f_N = f_I / K_{N-I}$ and $f_U = K_{I-U} \cdot f_I$, we can write the next expression as a function of the unique unknown magnitude, f_I:

$$n \cdot K_{I-In}{}^n \cdot K_{N-I} \cdot P^{n-1} \cdot f_I^n + (1 + K_{N-I} + K_{N-I} \cdot K_{I-U}) \cdot f_I - K_{N-I} = 0. \tag{7}$$

Therefore, by solving Eq. (7) all the thermodynamic information of the system can be deduced. In order to obtain the value of f_I we have applied a numerical approach, the Newton's method, commonly used to solve potential equations of the general formula $g(x_n) = 0$. This is an iterative method, where the initial estimate (x_n) progressively approaches the correct value according to:

$$x_{n+1} = x_n - \frac{g(x_n)}{g'(x_n)} \tag{8}$$

where x_{n+1} represents the value of the tangent line to the $g(x_n)$ function at x_n. We can confirm that 10 calculations are enough for a precise definition of the f_i value.

To complete the equations of this model it is also necessary to define the heat capacities of the four conformational states, always defined as a linear function of temperature:

$$\begin{aligned} C_{pN} &= a + b \cdot T \quad \text{Native state} \\ C_{pU} &= c + d \cdot T \quad \text{Unfolded state} \\ C_{pIn} &= h + i \cdot T \quad \text{Oligomeric intermediate state} \\ C_{pI} &= p + q \cdot T \quad \text{Intermediate state.} \end{aligned} \tag{9}$$

To define the enthalpy values for every involved process, reference temperatures T_{N-I}, T_{I-U} and T_{I-In}, related to the enthalpy values $\Delta H_{N-I}(T_{N-I})$, $\Delta H_{I-U}(T_{I-U})$ and $\Delta H_{I-In}(T_{I-In})$ are considered:

$$\begin{aligned} \Delta H_{N-I} &= \Delta H_{N-I}(T_{N-I})((p-a)\cdot(T-T_{N-I})) + \left(\frac{(q-b)\cdot\left(T^2-T_I^2\right)}{2}\right) \\ \Delta H_{I-U} &= \Delta H_{I-U}(T_{I-U}) + ((p-c)\cdot(T-T_{I-U})) + \left(\frac{(q-d)\cdot\left(T^2-T_{I-U}^2\right)}{2}\right) \\ \Delta H_{I-In} &= \Delta H_{I-In}(T_{I-In}) + ((h-p)\cdot(T-T_{I-In})) + \left(\frac{(i-q)\cdot\left(T^2-T_{I-In}^2\right)}{2}\right). \end{aligned} \tag{10}$$

In a similar way, changes in entropy can be also estimated from the relationship $dS = {}^{dH}/_{T} = C_p \cdot {}^{d,T}/_{T}$, giving place to the next equations:

$$\begin{aligned} \Delta S_{N-I} &= \Delta S_{N-I}(T_{N-I}) + \left((p-a)\cdot In\left({}^{T}/_{T_{N-I}}\right)\right) + ((q-b)\cdot(T-T_{N-I})) \\ \Delta S_{I-U} &= \Delta S_{I-U}(T_{I-U}) + \left((p-c)\cdot In\left({}^{T}/_{T_{I-U}}\right)\right) + ((q-d)\cdot(T-T_{I-U})) \\ \Delta S_{I-In} &= \Delta S_{I-In}(T_{I-In}) + \left((h-p)\cdot In\left({}^{T}/_{T_{I-In}}\right)\right) + ((i-q)\cdot(T-T_{I-In})). \end{aligned} \tag{11}$$

In this case, $\Delta S_{N-I}(T_{N-I})$, $\Delta S_{I-U}(T_{I-U})$ and $\Delta S_{I-In}(T_{I-In})$ values are defined by:

$$\begin{aligned} \Delta S_{N-I}(T_{N-I}) &= \frac{\Delta H_{N-I}(T_{N-I})}{T_{N-I}} \\ \Delta S_{I-U}(T_{I-U}) &= \frac{\Delta H_{I-U}(T_{I-U})}{T_{I-U}} \\ \Delta S_{I-In}(T_{I-In}) &= \frac{\Delta H_{I-In}(T_{I-In})}{T_{I-In}} + R\cdot In\left(\frac{2\cdot(1/2)^{1/n}\cdot P^{1/n}}{n^{1/n}\cdot P}\right). \end{aligned} \tag{12}$$

From the known equations $\Delta G = \Delta H - T\cdot\Delta S$ and $\Delta G = -RTlnK$, the values of equilibrium constants and populations can be estimated as a function of temperature. Finally, the global enthalpy change of the unfolding process is expressed by the sum of each of the enthalpies of the different states, weighted by their respective populations:

$$\Delta H = \Delta H_{N-I}\cdot f_I + (\Delta H_{N-I} + \Delta H_{I-U})\cdot f_U + (\Delta H_{I-U} + \Delta H_{I-In})\cdot f_{In}. \tag{13}$$

The global heat capacity of the process, which is measured experimentally, corresponds to the heat capacity of the native state plus the enthalpy dependence on the temperature upon unfolding, as indicated by the relation $C_p = C_{pN} + d\Delta H/dT$. Such function has been used to achieve the non-linear analysis of C_p *vs* T experimental data. The parameters to be calculated from these procedures are the $\Delta H_{N-I}(T_{N-I})$, $\Delta H_{I-U}(T_{I-U})$ and $\Delta H_{I-In}(T_{I-In})$ enthalpy values and the respective T_{N-I}, T_{I-U} and T_{I-In} mid-point temperatures, as well as the four linear C_{pX} functions defined by Eq. (9). When a multiple analysis was done, including several traces obtained at different concentrations of protein, the concentration-dependent thermodynamic magnitudes of the association equilibrium $I \rightleftarrows (1/n)\ I_n$ were calculated at a reference concentration of 100 μM. Calculations were made using SigmaPlot 2000 (Systat Software Inc.).

3. Results and discussion

We carried out DSC experiments in 50 mM potassium phosphate pH 7.5 at a heating rate of 1.5 $K\cdot min^{-1}$ and a set of protein concentrations ranging from 40 μM to 727 μM (Fig. 1). As it has been previously found for PSD95-PDZ3$^{302-402}$ [7] (Fig. S1) calorimetric traces show two well-separated endotherms shifting to opposite directions with protein concentration. So, the first endotherm moves towards low temperatures whereas the second does to high ones, being this shift related to association phenomena, where the first endotherm reflects an increase in the final state association and the second one the dissociation. Thus, in a three-state model this indicates a higher association stoichiometry for the intermediate state with respect to both, the native and the unfolded ones [16–18]. However, a significant difference concerning to the shape of the traces is observed between PSD95-PDZ3$^{302-392}$ and PSD95-PDZ3$^{302-402}$, being sharper in the first case.

DSC experiments were done by routinely heating the protein samples until 110 °C, which may originate high-temperature irreversible phenomena [19]. Thus, reversibility was tested by performing several experiments where reheating was checked after stopping the temperature scan at different temperatures (43 °C, 45 °C, 50 °C and 100 °C). As observed in Fig. S2, the shape of the reheated traces does not change. It is important to notice that heating above 70 °C decreases reversibility dramatically for almost all mesophilic proteins since some degradation of their chemical structure takes place [20]. Here, the reversibility of the first transition becomes lower as the stopping temperature increases, which indicates that some irreversible processes will take place between the two transitions. Thus, although some irreversible process can be coupled to the unfolding transition, this can still be seen as a cooperative and reversible process. This complies with the assumption that, if the temperature-induced unfolding takes place much faster than the unfolded protein aggregation, thermodynamics can be applied to the data analysis even if reversibility does not reach the 100% of the process [21]. In addition, we performed DSC experiments at a single protein concentration, 172 μM, but at different heating rates, ranging from 0.25 to 2.0 $K\cdot min^{-1}$ (Fig. S3), to decipher the extension of any

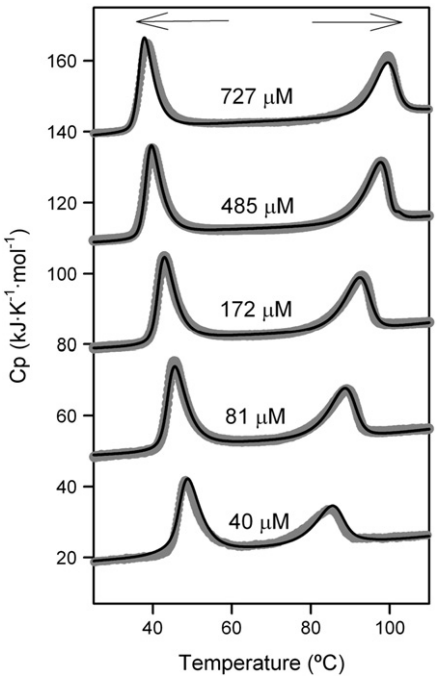

Fig. 1. Thermal unfolding experiments of PSD95-PDZ3$^{302-392}$ obtained by DSC as a function of the protein concentration (indicated on each curve). Experimental points are represented in gray circles whilst black solid lines represent the best fitting to the three-state model, including an intermediate which is self-associated.

Table 1
Thermodynamic parameters of the thermal unfolding of PSD95-PDZ3$^{302-392}$ in 50 mM potassium phosphate pH 7.5 obtained from the analysis of DSC experiments.

T_{N-I} (°C)	$\Delta H_{N-I}(T_{N-I})$ kJ·mol^{-1}	$\Delta G_{N-I}(298)$ kJ·mol^{-1}	T_{I-U} (°C)	$\Delta H_{I-U}(T_{I-U})$ kJ·mol^{-1}	$\Delta G_{I-U}(298)$ kJ·mol^{-1}	T_{I-In} (°C)	$\Delta H_{I-In}(T_{I-In})$ kJ·mol^{-1}	$\Delta G_{I-In}(343)$ kJ·mol^{-1}	$\Delta G_{N-U}(298)$ kJ·mol^{-1}
52 ± 3	250 ± 20	28 ± 8	79 ± 3	215 ± 10	17 ± 6	124.6 ± 4	−135 ± 15	−27 ± 5	28 ± 10

changes in curve shape that could be related to kinetic phenomena occurring during unfolding, which would therefore preclude thermodynamic analysis. We observed a slight displacement of the traces that shift towards high temperatures when the heating rate increases, in agreement with the mentioned irreversible phenomena. Nevertheless, we do not observe changes in shape and/or area, which indicates that the thermodynamic information derived from these traces will not be too much affected, among experimental errors, by kinetic processes. Additionally, reversibility was also checked by CD under the same buffer conditions and at 30 μM protein concentration. The far-UV spectra of PSD95-PDZ3$^{302-392}$ native state are recovered after cooling down a protein solution heated up to 98 °C (temperature enough to achieve a fully unfolded state according to DSC at this protein concentration) (Fig. S4). Hence, all these reversibility tests show that the thermal denaturation of PSD95-PDZ3$^{302-392}$ at the studied conditions is a reversible process that can be analyzed by using a thermodynamic model.

As mentioned above, the similar behavior observed between the DSC traces corresponding to PSD95-PDZ3$^{302-392}$ and those previously obtained for PSD95-PDZ3$^{302-402}$ [7] as a function of protein concentration suggests the presence of an intermediate state with higher stoichiometry than the native (N) and the unfolded (U) states. By also considering that the N state of PSD95-PDZ3$^{302-392}$ is monomeric, as shown by DLS analysis (see below), in a first attempt, fitting sessions were carried out using the most simple model with the presence of three states ($N \rightleftarrows I_n \rightleftarrows U$) where the intermediate state associates with n stoichiometry, as previously described for PSD95-PDZ3$^{302-402}$ [7]. Nevertheless, convergence was difficult to achieve and, even when successful, the traces displayed different shapes and wrongly split between transitions, so the low quality of the results clearly indicates that in this case such model is not suitable for thermodynamic analysis. Taking into account the association phenomena described above, we decided to explore an alternative and more complex situation where a monomeric intermediate state is included. In such situation, this monomeric intermediate associates, thus giving place to three different conformational states plus the association of one of them. After a global analysis, we attained a full description of the experimental traces obtained at different protein concentrations, as shown in Fig. 1. As it was done previously for PSD95-PDZ3$^{302-402}$ [7] we assumed common heat-capacity functions for the N, I, I_n and U states, as well as the thermodynamic parameters corresponding to the association equilibrium of the intermediate. The enthalpies and mid-point temperatures of the other equilibria were obtained separately for every DSC trace, being averaged later. The error interval for the unfolding parameters corresponding to the $N \rightleftarrows I$ and $I \rightleftarrows U$ equilibria was estimated from the scattering of these averaged results. Regarding the association stoichiometry of the intermediate, n, in a first attempt we allowed it to float in the global analysis, obtaining a value of $n = 2.8$, which indicates that trimers would be the most probable intermediate-associated species. Additionally, as shown in Fig. S5, the global analyses with n values of 2, 4 and 5 were also achieved. In the case of $n = 2$ the analysis converges nicely except for the trace corresponding to 40 μM of protein which barely deviates from the experimental data. Moreover, the analyses with $n = 4$ and especially $n = 5$ show a lower quality in almost the complete set of the traces than the corresponding one to $n = 3$. Thus, apart from the tendency to reach a value of $n = 2.8$ when such parameter keeps floating upon the fit, these results suggest that $n = 3$ can be considered as the best stoichiometry for the analysis achieved in a global way. Taking this into account, values collected in Table 1 from the fitting shown in Fig. 1 have been estimated from a fixed value of $n = 3$.

It would be interesting to point out that, despite the application of DSC in characterizing the thermal properties of proteins in solution has been extensively used [21,22] and it allows us to directly measure the effects related to inter and intra-molecular interactions as a function of the temperature, the thermodynamic analysis of the experimental traces is in some cases a hard challenge to achieve. Thus, whilst the unfolding process of a two state protein can be easily analyzed by using a simple model, the presence of more complex unfolding transitions requires the definition of some additional parameters due to the presence of one or several intermediates [23]. Moreover, in those cases where experimental conditions allow the observation of all the transitions occurring between N and U states, it is crucial to develop a global fit which can provide reasonable values for the different parameters, minimizing the associated errors. Our case represents an excellent example to consider the difficulty of applying a complex thermodynamic model in an efficient manner, obtaining results which can reproduce satisfactorily the experimental data.

By using the thermodynamic parameters of Table 1, the populations of these states as a function of temperature were simulated (Fig. 2) and compared with those of PSD95-PDZ3$^{302-402}$ [7]. In the case of PSD95-PDZ3$^{302-392}$ (panel A, Fig. 2) we observe that at the highest concentration of protein assayed, the trimeric intermediate populates almost 100% at the temperature interval 50–90 °C. Even at the lowest protein concentration, 90–100% population was reached in such temperature interval. The monomeric intermediate is maximally populated at the

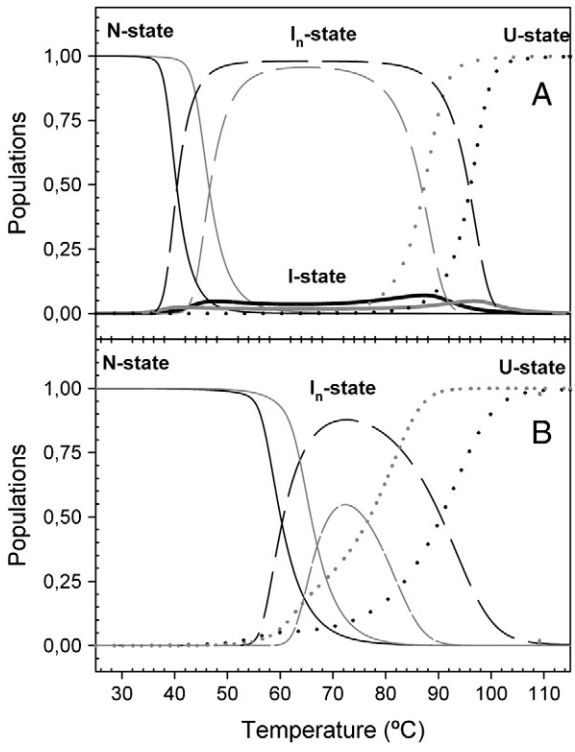

Fig. 2. Population distribution for the different states of the unfolding process of PSD95-PDZ3$^{302-392}$ (panel A) and PSD95-PDZ3 (panel B), at the two used concentration values: 40 μM (gray) and 727 μM (black).

flanking temperatures of this interval. This suggests that before and after the association phenomena ($I \rightleftarrows I_n$), a sequential unfolding pathway ($N \rightleftarrows I$ and $I \rightleftarrows U$) including at least one conformational change must occur. Surprisingly, despite the need of including the monomeric intermediate, it does not populate more than 10% at any temperature. However, in the case of PSD95-PDZ3$^{302–402}$ the highest population found for the intermediate at low protein concentration (40 μM) corresponds to 50%, being also narrower the corresponding temperature interval, 65 °C to 85 °C (panel B, Fig. 2). Hence, the analysis of Fig. 2 suggests that deletion of this α-helix stabilizes the oligomeric intermediate state, since it populates in a wider temperature range and in a higher percentage than in the case of PSD95-PDZ3$^{302–402}$ [7].

To get experimental evidence of the association phenomena observed in the DSC fitting analysis, we also performed DLS experiments under the same experimental conditions. We heated up PSD95-PDZ3$^{302–392}$ samples at 727 μM from 20 to 60 °C at a heating rate of 1 K·min^{-1}. At 20 °C we observe a single species with hydrodynamic radius $R_h = 1.8$ nm, determined as a monomer according to the molecular weight calculation module included in the software of the instrument, as described in the Materials and methods section. Monomers disappear from the solution at roughly 40 °C, emerging other species of higher sizes (Fig. 3A). These results qualitatively agree with the DSC population analysis (Fig. 2) but we did not find evidence of any trimeric species. Moreover, between 34 °C and 38 °C monomers coexist with bigger particles (6 nm), which could correspond to a molecular size of around 20 monomers. From 40 °C, monomer species disappears and, together with the 6 nm species, a quite bigger one of 24 nm emerges. Similarly to the 6 nm species, due to the large size of the 24 nm species, it is possible that the shape differs from that of a globular protein, making difficult to estimate accurately the corresponding molecular weight. On the basis of these results, we attempted an analysis of DSC traces setting association stoichiometry to $n = 20$. Fitting sessions did not give successful results so, perhaps association processes are even more complex than the suggested scheme, including additional equilibria, as the inter-association of trimers. Furthermore, we have checked the possible presence of an associated intermediate, by the DLS analysis of a 40 μM sample, which results in an association phenomena above 50 °C (Fig. 3B), again predicted by DSC (Fig. 2).

In summary, even though the simplest model that can explain data should be chosen when an analysis is performed, we cannot discard the possibility of having an even more complex behavior, in which oligomerisation events result from a mixture of dimers, trimers or other oligomers. From a global view of DLS and DSC results, it is revealed that DLS experiments do not show the stoichiometry derived from calorimetric analysis with a value of $n = 3$, indicating that such stoichiometry could be higher and would include different association states. Nevertheless, these two different techniques do not provide opposite results. Moreover, they inform about different aspects of the process, where the value of $n = 3$ obtained from DSC data would represent an average between the different species observed by DLS.

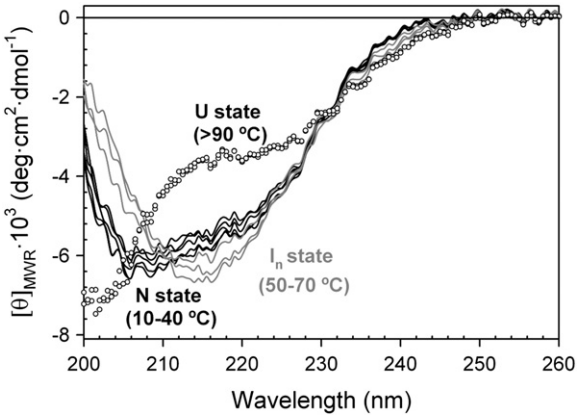

Fig. 4. CD temperature scans of PSD95-PDZ3$^{302–392}$ obtained at 30 μM. Data collection was performed between 10 and 98 °C in 10 °C intervals. Spectra in the ranges 10 °C–40 °C (N-state), 50 °C–70 °C (I and I_n states) and upper 90 °C (U state) are represented in black solid lines, gray solid lines and circles, respectively.

To get an approach of the conformational nature of the states of PSD95-PDZ3$^{302–392}$, we have collected some CD spectra of a 30 μM sample at different temperatures, under the same buffer conditions. Fig. 4 clearly shows three types of spectra within roughly the temperature intervals including the maximal population of every state (Fig. 2). In the interval 10–40 °C we observed the spectra of the native state, between 50 and 70 °C corresponding to the intermediate and, finally, above 90 °C we obtained the spectra corresponding to the unfolded state. The shape analysis of the CD spectra collection shows that the intermediate displays higher β-sheet content than the native state, as it is reflected by the minimum at 217 nm, whereas the unfolded state develops a typical spectrum with a minimum at 200 nm. It seems that some residual structure still remains at 98 °C since, in the region 210–225 nm, where helices and strands are optically active, ellipticity does not fully disappear. However, DSC experiments clearly show that at this low protein concentration the protein is unfolded at 98 °C (Fig. 1).

In order to deepen in the nature of the conformational transition leading to a higher β-sheet content in the oligomeric intermediate, as found by CD, we performed some FTIR analysis at 25 °C and 60 °C, where the native and the oligomeric intermediate states are mostly populated respectively. Band deconvolution of both amide I′ spectra generated six main-bands, centered at around 1680, 1670, 1660, 1650,

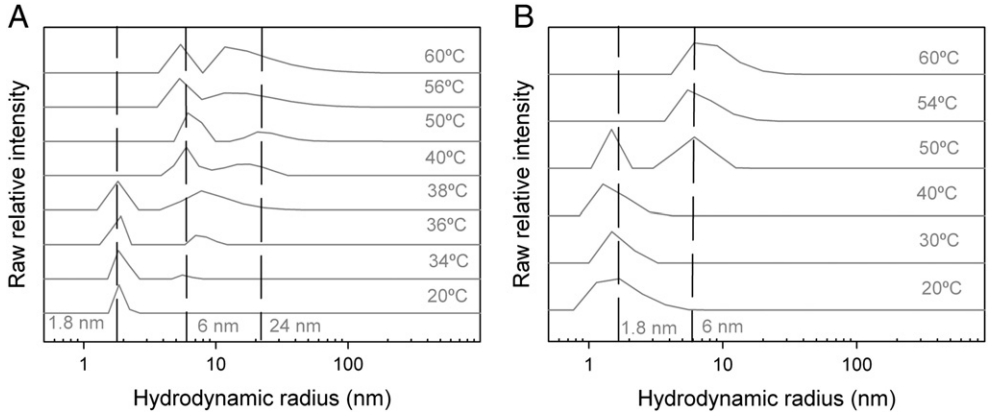

Fig. 3. Temperature scans of PSD95-PDZ3$^{302–392}$, followed by DLS from 20 °C to 60 °C at a scan rate of 1 K·min^{-1} at 727 μM (A) and 40 μM (B).

1640 and 1630 cm^{-1}; as well as three-minor bands at around 1690, 1620 and 1605 cm^{-1} (Fig. 5). Concerning regular secondary structures, α-helix content is reflected by the 1650 cm^{-1} band and contributes a 14% to the area of the native spectrum; β-sheet content is not as straightforward to be assigned because three components occur: 1640 cm^{-1} (native and highly flexible) contributing 21%, 1630 cm^{-1} (native) contributing 22%, and 1620 cm^{-1} (associated) contributing 6% (Fig. 5A) [14]. Although the α-content slightly decreases, the percentages of the β-components dramatically change in the oligomeric intermediate state (Fig. 5B). The huge increase of the 1620 cm^{-1} band (from 6% to 29%) is generated at the expense of the rest of the bands and it is indicative of a conformational transition from the native state to a structure where a compact β-sheet predominates. Such compact β-sheet should be present in the monomeric intermediate state, being responsible of the intermolecular hydrogen bonding network leading to association.

In summary, our calorimetric analysis shows that the third PDZ domain of PSD95 protein under study presents a complex thermodynamic behavior, including the presence of a very stable oligomeric intermediate. Considering that our construct essentially includes the secondary structure elements of a canonical PDZ domain, the presence of an intermediate is unexceptional since previous studies have reported the presence of folding intermediates in PDZ domains [24,25]. Besides, the comparison of the behavior of both constructs of the domain, PSD95-PDZ3 and PSD95-PDZ3$^{302–392}$, reveals that the presence of the extra-helix α3 makes somewhat simpler the unfolding process. In opposition, most examples in bibliography show that proteins of small size usually follow a simple two-state mechanism as, for example, SH3 or GYF domains [26,27], which comprise 7–8 kDa [28]. As molecular weight increases, proteins tend to present more complex conformational equilibria, displaying association phenomena [29] and/or intermediates [30]. Our data constitute a singular case in protein folding, maybe due to the nature of these domains, since their conformational plasticity could be used by nature to perform its function of connecting diverse processes in the cell. Indeed, it has been demonstrated that by removing the α3-helix, a dynamic allosteric regulation mechanism is detected for the PSD95-PDZ3 domain, which results in the loss of affinity to its ligands [6]. Besides, such helix contains a tyrosine residue which can be phosphorylated [31]. Phosphorylation has also been proven to regulate binding since that phosphate group disrupts the proper packing of the α3-helix onto the domain [32]. Hence, the conformational plasticity of the domain including the different ways of regulation would be a feature that likely allows its multiple functionality.

4. Conclusions

The detailed calorimetric analysis of the unfolding behavior of the third PDZ domain of PSD95 in the absence of its third α-helix shows a more complex situation than the previously observed for the PDZ3-PSD95$^{302–402}$ domain. Thus, when the helix is removed, the oligomeric intermediate becomes more stable than the observed for the construct containing the α3-helix. These data, supported by CD, DLS and FTIR information, suggest that, despite the universality of this three-state unfolding behavior observed for PDZ domains, making the amino acidic sequence of PDZ3-PSD95 shorter by deletion of this linking element introduces a higher degree of complexity in its unfolding process, constituting a rare case in protein folding.

Abbreviations

PDZ	postsynaptic density protein-95/disks large/zonula occludens-1
PSD-95	postsynaptic density protein-95
DSC	differential scanning calorimetry
FTIR	Fourier transform infrared spectroscopy
DLS	dynamic light scattering
CD	circular dichroism

Acknowledgments

This research was supported by grants CVI-05915, from the Andalusian Regional Government; BIO2009-13261-C02-01 and BIO2012-3922-C0201 from the Spanish Ministry of Science and Education and FEDER; FIS10-00975, from the Instituto de Salud Carlos III and SGR2009-00761, from Generalitat de Catalunya. J.M.C. received a postdoctoral contract from the Spanish Ministry of Science and Education. M.M.-A. is supported by a PIF (UAB) fellowship. We thank our colleague Dr. Salvador Casares Atienza for revising our English text.

Appendix A. Supplementary data

Supporting material contains Figs. S1–S5. They represent the comparison of the DSC traces obtained for PSD95-PDZ3$^{302–402}$ and PSD95-PDZ3$^{302–392}$ domains (Fig. S1) and the DSC (Figs. S2 and S3) and CD (Fig. S4) experiments performed to test the reversibility of the process As mentioned in the text, this is crucial to justify the analysis based on

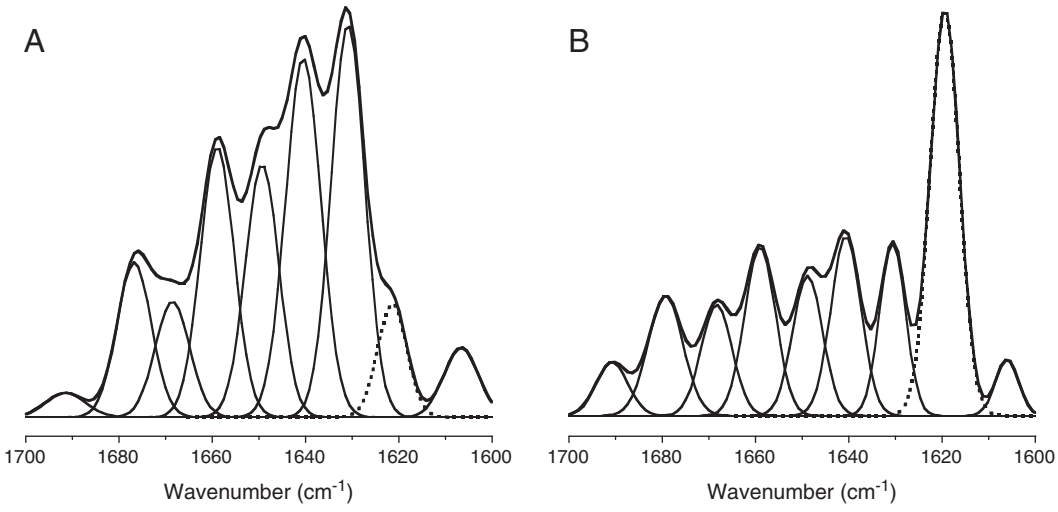

Fig. 5. Deconvolution of FTIR spectra at 25 °C (A) and 60 °C (B). The band represented by a dotted line represents the one having the major change upon incubation at 60 °C for 5 min (centered at around 1620 cm^{-1}).

thermodynamic models. Fig. S5 shows the comparison between the global DSC data analysis carried out by using different n values. Supplementary data to this article can be found online at http://dx.doi.org/10.1016/j.bpc.2013.10.005.

References

[1] A.-L. Barabasi, R. Albert, Emergence of scaling in random networks, Science 286 (1999) 509–512.
[2] A.S. Fanning, J.M. Anderson, Protein–protein interactions: PDZ domain networks, Curr. Biol. 6 (1996) 1385–1388.
[3] W. Feng, M. Zhang, Organization and dynamics of PDZ-domain-related supramodules in the postsynaptic density, Nat. Rev. Neurosci. 10 (2009) 87–99.
[4] J. Zhang, S.M. Lewis, B. Kuhlman, Andrew L. Lee, Supertertiary structure of the MAGUK core from PSD-95, Structure 21 (2013) 402–413.
[5] D.A. Doyle, A. Lee, J. Lewis, E. Kim, M. Sheng, R. MacKinnon, Crystal structures of a complexed and peptide-free membrane protein-binding domain: molecular basis of peptide recognition by PDZ, Cell 85 (1996) 1067–1076.
[6] C.M. Petit, J. Zhang, P.J. Sapienza, E.J. Fuentes, A.L. Lee, Hidden dynamic allostery in a PDZ domain, Proc. Natl. Acad. Sci. 106 (2009) 18249–18254.
[7] J. Murciano-Calles, E.S. Cobos, P.L. Mateo, A. Camara-Artigas, J.C. Martinez, An oligomeric equilibrium intermediate as the precursory nucleus of globular and fibrillar supramacromolecular assemblies in a PDZ domain, Biophys. J. 99 (2010) 263–272.
[8] E. Freire, D.T. Haynie, D. Xie, Molecular Basis of Cooperativity in Protein Folding IV, Core: A General Cooperative Folding Model, Proteins: Structure, Function, and Bioinformatics, 171993. 111–123.
[9] A. Cámara-Artigas, J. Murciano-Calles, J.A. Gavira, E.S. Cobos, J.C. Martínez, Novel conformational aspects of the third PDZ domain of the neuronal post-synaptic density-95 protein revealed from two 1.4 Å X-ray structures, J. Struct. Biol. 170 (2010) 565–569.
[10] S.C. Gill, P.H. von Hippel, Calculation of protein extinction coefficients from amino acid sequence data, Anal. Biochem. 182 (1989) 319–326.
[11] A.R. Viguera, J.C. Martinez, V.V. Filimonov, P.L. Mateo, L. Serrano, Thermodynamic and kinetic analysis of the SH3 domain of spectrin shows a two-state folding transition, Biochemistry 33 (1994) 2142–2150.
[12] E.S. Cobos, M. Iglesias-Bexiga, J. Ruiz-Sanz, P.L. Mateo, I. Luque, J.C. Martinez, Thermodynamic characterization of the folding equilibrium of the human Nedd4-WW4 domain: at the frontiers of cooperative folding, Biochemistry 48 (2009) 8712–8720.
[13] E.S. Cobos, M.T. Pisabarro, M.C. Vega, E. Lacroix, L. Serrano, J. Ruiz-Sanz, J.C. Martinez, A miniprotein scaffold used to assemble the polyproline II binding epitope recognized by SH3 domains, J. Mol. Biol. 342 (2004) 355–365.
[14] M. Marin-Argany, Adela M. Candel, J. Murciano-Calles, Jose C. Martinez, S. Villegas, The interconversion between a flexible-sheet and a fibril-arrangement constitutes the main conformational event during misfolding of PSD95-PDZ3 domain, Biophys. J. 103 (2012) 738–747.
[15] J. Murciano-Calles, E.S. Cobos, P.L. Mateo, A. Camara-Artigas, J.C. Martinez, A comparative analysis of the folding and misfolding pathways of the third PDZ domain of PSD95 investigated under different pH conditions, Biophys. Chem. 158 (2011) 104–110.
[16] I.s. Burgos, S.A. Dassie, G.D. Fidelio, Thermodynamic model for the analysis of calorimetric data of oligomeric proteins, J. Phys. Chem. B 112 (2008) 14325–14333.
[17] V.V. Filimonov, V.V. Rogov, Reversible association of the equilibrium unfolding intermediate of [lambda] Cro repressor, J. Mol. Biol. 255 (1996) 767–777.
[18] J. Ruiz-Sanz, V.V. Filimonov, E. Christodoulou, C.E. Vorgias, P.L. Mateo, Thermodynamic analysis of the unfolding and stability of the dimeric DNA-binding protein HU from the hyperthermophilic eubacterium Thermotoga maritima and its E34D mutant, Eur. J. Biochem. 271 (2004) 1497–1507.
[19] J.C. Martinez, V.V. Filimonov, P.L. Mateo, G. Schreiber, A.R. Fersht, A calorimetric study of the thermal stability of barstar and its interaction with barnase, Biochemistry 34 (1995) 5224–5233.
[20] G.P. Privalov, P.L. Privalov, Michael, Problems and prospects in microcalorimetry of biological macromolecules, Methods in Enzymology, Academic Press, 2000.
[21] P. Privalov, Microcalorimetry of proteins and their complexes, Protein Structure, Stability, and Interactions, Humana Press, 2009, pp. 1–39.
[22] C.M. Johnson, Differential scanning calorimetry as a tool for protein folding and stability, Arch. Biochem. Biophys. 531 (2013) 100–109.
[23] J.C. Martinez, E.S. Cobos, I. Luque, J. Ruiz-Sanz, Differential scanning calorimetry: thermodynamic analysis of the unfolding transitions of proteins, domains and peptidic fragments by using equilibrium models, in: E.C. Walter (Ed.), Protein Folding, 2010.
[24] C.N. Chi, S. Gianni, N. Calosci, C. Travaglini-Allocatelli, K. Engstrom, P. Jemth, A conserved folding mechanism for PDZ domains, FEBS Lett. 581 (2007) 1109–1113.
[25] S. Gianni, N. Calosci, J.M. Aelen, G.W. Vuister, M. Brunori, C. Travaglini-Allocatelli, Kinetic folding mechanism of PDZ2 from PTP-BL, Protein Eng. Des. Sel. 18 (2005) 389–395.
[26] M. Andujar-Sanchez, E.S. Cobos, I. Luque, J.C. Martinez, Thermodynamic impact of embedded water molecules in the unfolding of human CD2BP2-GYF domain, J. Phys. Chem. B 116 (2012) 7168–7175.
[27] E.S. Cobos, V.V. Filimonov, M.C. Vega, P.L. Mateo, L. Serrano, J.C. Martinez, A thermodynamic and kinetic analysis of the folding pathway of an SH3 domain entropically stabilised by a redesigned hydrophobic core, J. Mol. Biol. 328 (2003) 221–233.
[28] S.E. Jackson, How do small single-domain proteins fold? Fold. Des. 3 (1998) R81–R91.
[29] E. Rennella, T. Cutuil, P. Schanda, I. Ayala, F. Gabel, V. Forge, A. Corazza, G. Esposito, B. Brutscher, Oligomeric states along the folding pathways of $I^2$2-microglobulin: kinetics, thermodynamics, and structure, J. Mol. Biol. 425 (2013) 2722–2736.
[30] M. Tsytlonok, L.S. Itzhaki, The how's and why's of protein folding intermediates, Arch. Biochem. Biophys. 531 (2013) 14–23.
[31] B.A. Ballif, G.R. Carey, S.R. Sunyaev, S.P. Gygi, Large-scale identification and evolution indexing of tyrosine phosphorylation sites from murine brain, J. Proteome Res. 7 (2007) 311–318.
[32] J. Zhang, C.M. Petit, D.S. King, A.L. Lee, Phosphorylation of a PDZ domain extension modulates binding affinity and interdomain interactions in postsynaptic density-95 (PSD-95) protein, a membrane-associated guanylate kinase (MAGUK), J. Biol. Chem. 286 (2011) 41776–41785.